

Supplementary Information

A Nonlinear Optical Crystal with Deep-ultraviolet Transparency and Appropriate Birefringence Achieved using π -Conjugation Confined $[B_3O_3F_4(OH)]^{2-}$

Tao Ouyang,^{a,b} Xu Chen,^{a,b} Shanshan Chen,^b Yanqiang Li,^b Xiaoying Shang,^{b*} Zhiyong Bai,^b Ningtao Jiang,^c Zhishuo Yan,^c Junhua Luo^b and Sangen Zhao^{b*}

^aCollege of Chemistry, Fuzhou University, Fuzhou 350116, China

^bState Key Laboratory of Structural Chemistry, Fujian Institute of Research on the Structure of Matter, Chinese Academy of Sciences, Fuzhou 350002, China

^cDepartment of Electrical and Computer Engineering, North Dakota State University, Fargo 58102, USA

CONTENTS

Single-Crystal Structure Determination.....	3
Powder X-Ray Diffraction.....	3
Elemental Analysis and Scanning Electron Microscope Mapping.....	3
UV-Vis-NIR Transmission Spectroscopy.....	4
Thermal Stability.....	4
FTIR Analysis	4
SHG Measurements.....	4
Birefringence Tests.....	5
Theoretical Calculations.....	6
Figure S1. The powder XRD of KBOFH.....	7
Figure S2. (a) The unexposed KBOFH single crystal. (b) KBOFH single crystal after exposed to the air for one week.	7
Figure S3. The PXRD patterns of KBOFH exposed in air for one week and two weeks.	8
Figure S4. Energy dispersive X-ray (EDX) analysis of KBOFH.....	8
Figure S5. The UV-Vis-NIR diffuse reflectance spectrum of KBOFH.	9
Figure S6. TG and DTA curves of KBOFH.	9
Figure S7. FTIR of KBOFH.	9
Figure S8 The thickness of the selected KBOFH single-crystal used for the birefringence measurement.....	10
Figure S9 Refractive index dispersion curves and the shortest phase-matching wavelength for KBOFH.....	10
Table S1. Crystallographic data and structural refinement for KBOFH.....	11
Table S2. Atomic coordinates ($\times 10^4$) and equivalent isotropic displacement parameters ($\text{\AA}^2 \times 10^3$) for KBOFH.....	12
Table S3. Anisotropic displacement parameters (\AA^2) for KBOFH.	14
Table S4. Selected bond distances (\AA) for KBOFH.	16
Table S5. Selected bond angles ($^\circ$) for $\text{K}_2\text{B}_3\text{O}_3\text{F}_4\text{OH}$	18
References	20

Single-Crystal Structure Determination.

A high-quality colorless crystal of $K_2B_3O_3F_4(OH)$ (KBOFH) was selected using an optical microscope for single-crystal X-ray diffraction (XRD) analysis. The diffraction data were collected by using graphite-monochromatized Cu $K\alpha$ radiation ($\lambda = 1.5418 \text{ \AA}$) at 293(2) K on an Rigaku Oxford diffractometer. The collection of the intensity data, cell refinement, and data reduction was carried out with the CrysAlisPro software (version 1.171.41.116a). Using Olex2,¹ the structure was solved with the SHELXS² structure solution program using Direct Methods and refined with the SHELXL³ refinement package using Least Squares minimisation. Final refinements include anisotropic displacement parameters. Both structures were verified by the ADDSYM algorithm from the program PLATON,⁴ and no higher symmetry was found. Details of crystal parameters, data collection, and structure refinement were summarized in Table S1. The atomic coordinates and equivalent isotropic displacement parameters were listed in Table S2. The anisotropic displacement parameters were listed in Table S3. Selected bond lengths and bond angles were presented in Table S4 and Table S5.

Powder X-Ray Diffraction.

Powder X-ray diffraction (PXRD) measurement for the sample of KBOFH was carried out with a Miniflex 600 diffractometer equipped with an incident beam monochromator set of Cu $K\alpha$ radiation ($\lambda = 1.5418 \text{ \AA}$), and the 2θ range of 5-50°, with a scan step width of 0.02° and a scanning rate of 0.15° min⁻¹.

Elemental Analysis and Scanning Electron Microscope Mapping.

The elemental analysis was performed on the Vario MICRO cube Elementar. In addition, the scanning electron microscope (SEM) elemental mapping on the KBOFH single crystal was collected on a field emission SEM (Hitachi SU8010).

UV-Vis-NIR Transmission Spectroscopy.

UV-Vis-NIR transmission spectral data were recorded at room temperature with a PerkinElmer Lamda-950 UV-Vis-NIR spectrophotometer. The scanned wavelength range was 200 nm to 800 nm using transparent bulk crystals obtained from natural growth.

Thermal Stability.

The thermal stability was investigated by the differential thermal analysis (DTA) on a simultaneous NETZSCH STA 449C thermal analyzer in an atmosphere of flowing N₂. About 6.24 mg KBOFH powders were placed into an Al₂O₃ crucible, and heated at a rate of 10 K·min⁻¹ from room temperature to 950 K (Figure S4). According to the thermogravimetry - differential thermal analysis (TG-DTA) curves of KBOFH, an endothermic peak appears at 550 K on the DTA curve and corresponds to the mass loss on the TG curve. The experimental weight loss (6.13%) corresponds exactly to the theory OH weight loss (6.75%), which indicated only one OH in the unit structure.

FTIR Analysis

Fourier transform infrared spectroscopy (FTIR) in the wavenumber range of 4000 - 675 cm⁻¹ was recorded on Thermo Nicolet 6700 (manufactured in the United States) infrared spectrometer.

SHG Measurements.

Powder SHG measurement: The powder SHG measurements were performed on a Q-switched Nd: YAG laser at the wavelength of 1064 nm. Polycrystalline samples of KBOFH were ground. The sample were pressed between glass slides and secured with

tape in 1-mm thick aluminum holders containing an 8-mm diameter hole. They were then placed into a light-tight box and irradiated with the laser. The intensity of the frequency-doubled output emitted from the samples was collected by a photomultiplier tube. Crystalline KH_2PO_4 (KDP) samples were also ground and used as references.

A monocrystalline SHG measurement: The SHG experiments were conducted on a home-built optical system operated in reflection geometry. A tunable femtosecond laser (pulse width: 70 fs; repetition frequency: 80 MHz; 710-920 nm, Mai Tai XF-1, Spectra-Physics) was used as the excitation source, which passes through a polarizing beamsplitter, an 800 nm half-wave plate, a dichroic mirror and an objective (50 \times , NA 0.8, Nikon) before interaction with samples. The same objective was used to collect the SHG signal. The spectrum was measured using a spectrometer (Princeton Instruments, SP2500) cooled by liquid nitrogen. All of the experiments were carried out at room temperature.

Birefringence Tests.

The birefringence of KBOFH was characterized by the polarized method under the polarized microscope (Nikon ECLIPSE LV100N POL) equipped with a Berek compensator. The wavelength of the light source was $\lambda = 550$ nm. The relative error is small enough because of the clear boundary lines of the first-, second- and third-order interference color. In order to improve the accuracy of the birefringence, small and transparent KBOFH crystals were chosen. The tested crystal planes were determined by single-crystal XRD diffraction. The formula for calculating the birefringence is listed below:^{5, 6}

$$R = |n_e - n_o| \times d = \Delta n \times d$$

Here, R represents the optical path difference, Δn is the birefringence, and d denotes the thickness of the tested crystal.

Theoretical Calculations.

The first-principles calculations were carried out with the CASTEP software,⁷ a plane-wave pseudopotential package⁸ on the basis of the density functional theory (DFT).⁹ The exchange-correlation energy was described by the generalized gradient approximation (GGA) scheme of the Perdew-Burke-Ernzerhof (PBE) functional, as implemented in the CASTEP code.¹⁰ Norm-conserving pseudopotentials were employed to simulate the ion-electron interactions for each atomic specie with following valence configurations: H 1s¹, B 2s² 2p¹, O 2s² 2p⁴, F 2s² 2p⁵, K 3s² 3p⁶ 4s¹.¹¹ A cutoff energy of 850 eV and the Monkhorst-Pack¹² k-point meshes ($2 \times 2 \times 7$) spacing about 0.02 Å⁻¹ in the Brillouin zone were chosen for the calculation. Considering that GGA-PBE usually severely underestimates the band gap, the HSE06 functional was employed to further calculate the band gap for KBOFH. Herein, all calculations were performed without the scissors operator.

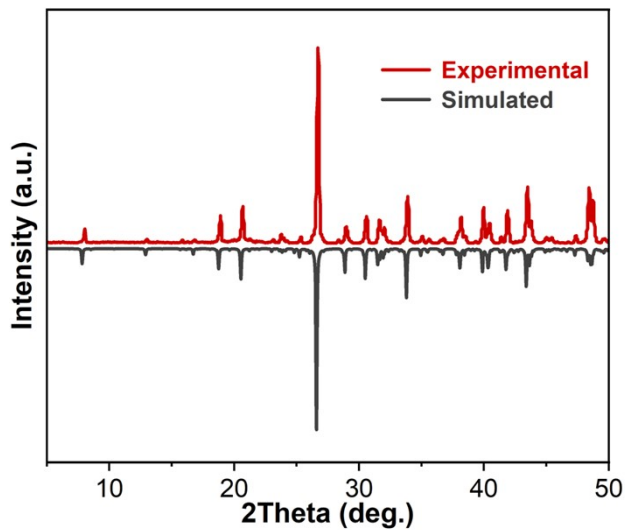


Figure S1. The powder XRD of KBOFH.

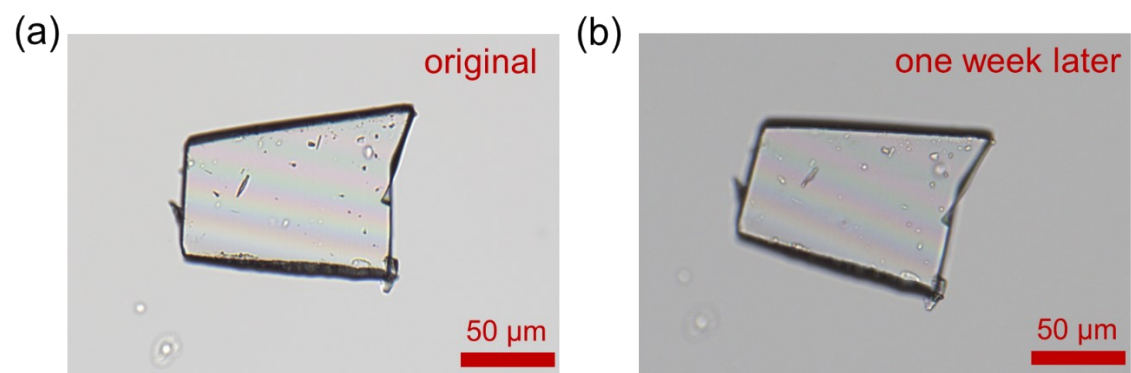


Figure S2. (a) The unexposed KBOFH single crystal. (b) KBOFH single crystal after exposed to the air for one week.

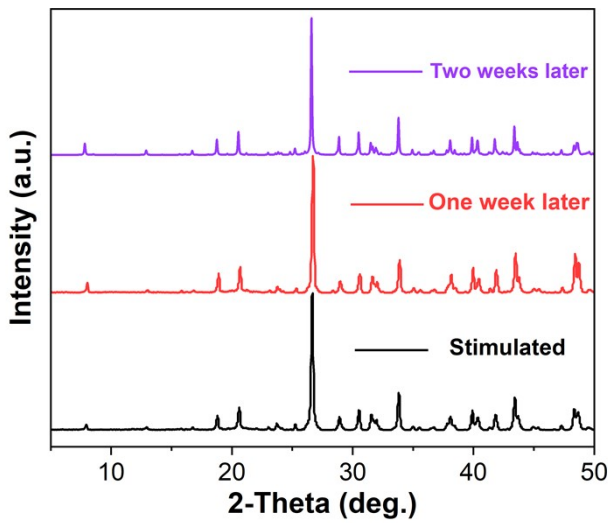


Figure S3. The PXRD patterns of KBOFH exposed in air for one week and two weeks.

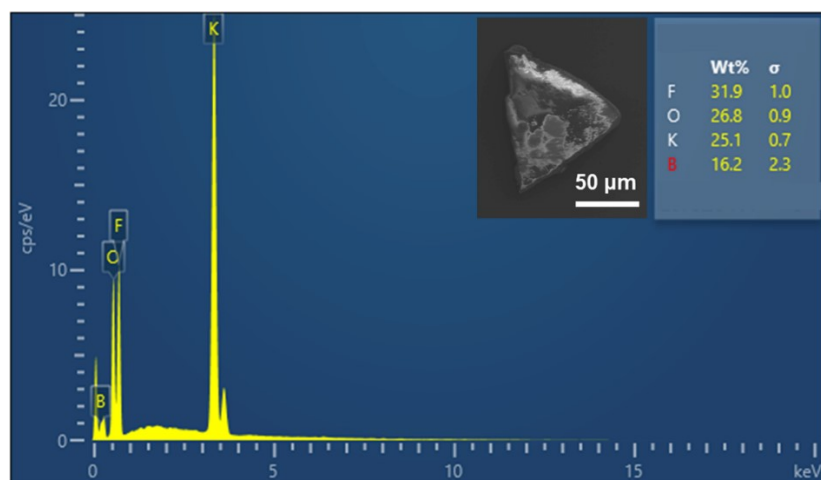


Figure S4. Energy dispersive X-ray (EDX) analysis of KBOFH.

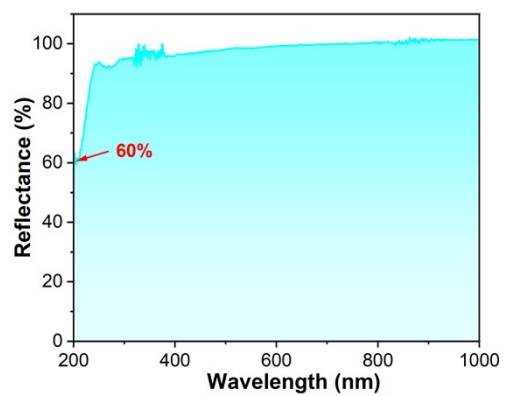


Figure S5. The UV-Vis-NIR diffuse reflectance spectrum of KBOFH.

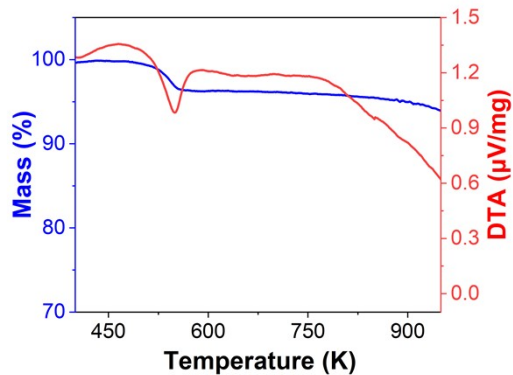


Figure S6. TG and DTA curves of KBOFH.

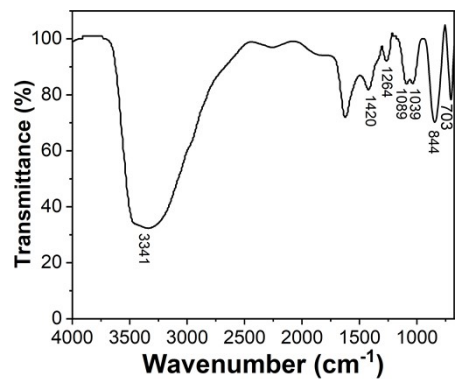


Figure S7. FTIR of KBOFH.

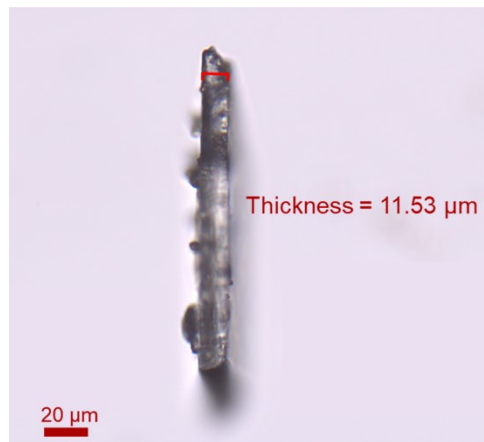


Figure S8 The thickness of the selected KBOFH single-crystal used for the birefringence measurement.

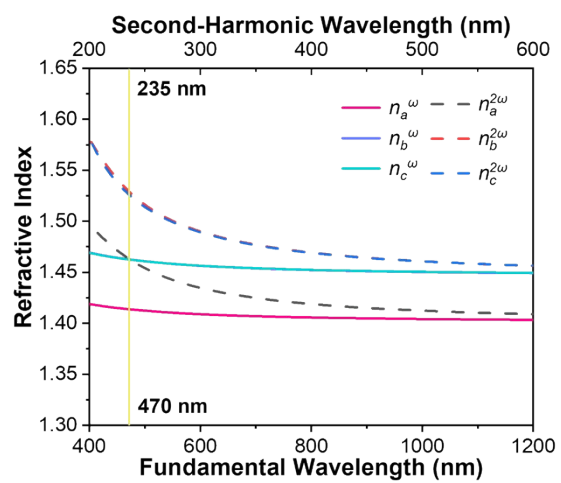


Figure S9 Refractive index dispersion curves and the shortest phase-matching wavelength for KBOFH.

Table S1. Crystallographic data and structural refinement for KBOFH.

Empirical formula	K ₂ B ₃ O ₃ F ₄ (OH)
Formula weight	251.64
Temperature/K	293.15
Crystal system	orthorhombic
Space group	<i>Ama2</i>
<i>a</i> /Å	25.9308(5)
<i>b</i> /Å	22.5853(4)
<i>c</i> /Å	7.46320(10)
$\alpha/^\circ$	90
$\beta/^\circ$	90
$\gamma/^\circ$	90
Volume/Å ³	4370.86(13)
<i>Z</i>	24
ρ (g/cm ³)	2.294
μ /mm ⁻¹	12.153
<i>F</i> (000)	2928
Radiation	Cu $K\alpha$ ($\lambda = 1.54184$)
2θ range for data collection/°	6.818 to 153.196
Index ranges	-32 ≤ <i>h</i> ≤ 29, -27 ≤ <i>k</i> ≤ 21, -9 ≤ <i>l</i> ≤ 8
Reflections collected	7457
Independent reflections	3271 ($R_{\text{int}} = 0.0236$, $R_{\text{sigma}} = 0.0339$)
Data/restraints/parameters	3271/20/398
Goodness-of-fit on <i>F</i> ²	1.060
Final <i>R</i> indexes ($I \geq 2\sigma(I)$) ^[a]	$R_1 = 0.0375$, $wR_2 = 0.1070$
Final <i>R</i> indexes (all data) ^[a]	$R_1 = 0.0407$, $wR_2 = 0.1097$
Largest diff. peak/hole (e Å ⁻³)	0.70/-0.51
Flack parameter	0.076(19)

[a] $R_1 = \sum ||F_o| - |F_c|| / \sum |F_o|$ and $wR_2 = [\sum w(F_o^2 - F_c^2)^2 / \sum wF_o^4]^{1/2}$ for $F_o^2 > 2\sigma(F_o^2)$.

Table S2. Atomic coordinates ($\times 10^4$) and equivalent isotropic displacement parameters ($\text{\AA}^2 \times 10^3$) for KBOFH.

Atom	x	y	z	$U(\text{eq})^{[\text{a}]}$
K1	5000	5000	8610(2)	29.0(4)
K2	4951.0(4)	8332.6(4)	8823.5(18)	30.5(3)
K3	5787.4(6)	8262.4(5)	14354(2)	47.6(4)
K4	7500	6689.4(5)	8159(3)	26.8(3)
K5	6630.8(4)	6668.6(4)	3498(2)	30.3(3)
K6	6687.0(4)	8275.0(4)	-1059.3(19)	30.9(3)
K7	8327.7(4)	9973.7(4)	3693(2)	29.8(3)
B1	5822.0(19)	4380(3)	2478(9)	26.0(11)
B2	5826.7(17)	4241(2)	5789(9)	21.6(11)
B3	5833.3(17)	5222(2)	4518(9)	23.7(12)
B4	5708(2)	7252(2)	10435(9)	32.2(12)
B5	6019.6(17)	7035(2)	7406(8)	24.5(10)
B6	5844.6(17)	6242(2)	9524(8)	23.7(11)
B7	7500	7654(3)	1929(13)	31.8(18)
B8	7335(3)	7944(4)	5038(16)	24(2)
B9	7500	8696(3)	2858(11)	20.6(14)
B10	7500	10575(3)	-57(12)	23.3(14)
B11	7500	10716(3)	-3398(11)	20.2(14)
B12	7500	9721(3)	-2095(12)	25.1(16)
O1	5828.2(12)	4022.4(12)	4015(5)	23.5(7)
O2	5830.0(11)	4877.1(14)	5978(5)	25.4(7)
O3	5839.0(13)	5833.8(15)	4675(6)	31.5(8)
O4	5825.7(14)	5009.5(16)	2820(6)	35.8(10)
O5	5836.1(14)	7438.2(13)	8690(6)	28.6(7)

O6	5896.1(15)	6414.8(15)	7791(6)	34.9(9)
O7	5835.8(12)	5644.9(14)	9816(6)	28.4(8)
O8	5805.3(12)	6638.1(14)	10868(6)	27.0(8)
O9	7500	7509(2)	3778(8)	30.9(11)
O10	7500	8536(2)	4616(8)	33.3(12)
O11	7500	9298(2)	2509(8)	31.0(11)
O12	7931.8(13)	10718.6(14)	1034(6)	46.9(9)
O13	7500	10932.6(18)	-1618(8)	26.5(10)
O14	7500	10075.4(19)	-3588(7)	27.5(10)
O15	7500	9116(2)	-2254(9)	35.6(12)
O16	7500	9947(2)	-424(8)	37.5(13)
F1	6245.4(13)	4227.6(14)	1336(6)	45.5(8)
F2	5381.4(12)	4231.4(14)	1391(5)	42.1(8)
F3	5380.7(11)	4016.6(12)	6749(5)	33.8(7)
F4	6257.6(11)	4003.8(12)	6783(5)	33.7(7)
F5	5963(2)	7600.3(17)	11716(6)	87.7(16)
F6	5170.5(17)	7343(2)	10715(9)	108(2)
F7	6569.9(11)	7070.2(17)	7238(7)	53.3(10)
F8	5835.4(10)	7166.6(13)	5651(5)	30.2(6)
F9	7072.3(15)	7391.9(14)	1023(6)	53.0(10)
F10	6771.0(19)	7978(3)	5151(11)	42.2(15)
F11	7500	7808.8(17)	6791(6)	29.7(9)
F12	7931.8(13)	10718.6(14)	1034(6)	46.9(9)
F13	7063.6(10)	10940.1(11)	-4357(5)	29.2(6)

[a] U_{eq} is defined as one-third of the trace of the orthogonalized U_{ij} tensor.

Table S3. Anisotropic displacement parameters (\AA^2) for KBOFH.

Atom	U11	U22	U33	U23	U13	U12
K1	28.2(6)	24.9(6)	34.1(10)	0	0	-0.2(4)
K2	29.8(5)	26.5(5)	35.2(8)	1.8(4)	-3.4(5)	-5.1(3)
K3	88.0(10)	23.8(5)	31.0(8)	-0.4(5)	4.3(6)	4.8(5)
K4	32.6(6)	19.1(6)	28.9(9)	3.8(6)	0	0
K5	30.0(4)	29.7(5)	31.1(8)	0.5(4)	1.5(5)	3.3(3)
K6	30.0(5)	27.4(5)	35.4(9)	-2.4(5)	-2.4(5)	3.8(3)
K7	29.6(5)	25.1(5)	34.6(6)	-4.5(4)	1.3(3)	1.9(3)
B1	42(3)	16(2)	20(3)	-1(2)	0(2)	-2.3(17)
B2	29(2)	13(2)	24(3)	-0.7(19)	-1(2)	-0.5(15)
B3	32(2)	19(3)	19(3)	1(2)	-0.8(19)	1.4(16)
B4	50(3)	22(3)	24(3)	3(2)	10(3)	12(2)
B5	28(2)	25(3)	21(3)	2(2)	0(2)	-3.8(18)
B6	28(2)	22(2)	21(3)	0(2)	-2.5(19)	0.6(16)
B7	55(5)	17(3)	23(4)	1(3)	0	0
B8	34(5)	20(4)	19(5)	1(4)	1(4)	-2(3)
B9	29(3)	14(3)	19(4)	4(3)	0	0
B10	38(3)	16(3)	16(4)	-1(3)	0	0
B11	31(3)	15(3)	15(4)	3(3)	0	0
B12	44(3)	12(3)	20(4)	1(3)	0	0
O1	40.1(15)	14.0(13)	16.6(17)	-2.4(13)	-2.9(14)	0.5(11)
O2	45.1(17)	13.8(14)	17.3(18)	-2.1(13)	0.1(13)	-1.1(11)
O3	61(2)	12.8(14)	21(2)	1.6(14)	-1.6(16)	-2.1(12)
O4	70(3)	18.0(18)	19(2)	2.2(15)	-0.9(16)	-2.5(13)
O5	46.9(16)	14.9(13)	23.9(19)	2.4(15)	3.6(12)	-0.6(13)
O6	70(2)	17.5(18)	17.1(18)	-0.1(15)	0.0(17)	-0.2(14)
O7	45.9(18)	17.1(15)	22.2(19)	2.9(14)	-3.0(14)	-1.5(11)

O8	41.0(18)	19.5(16)	21(2)	1.3(13)	1.0(14)	3.7(11)
O9	53(3)	17(2)	23(3)	-2.2(19)	0	0
O10	63(3)	19(2)	18(3)	0(2)	0	0
O11	53(3)	18(2)	22(3)	4(2)	0	0
O12	46(3)	16(2)	19(3)	0.5(17)	0	0
O13	45(2)	13.8(18)	21(2)	0.8(19)	0	0
O14	49(3)	14.3(19)	20(2)	-0.5(19)	0	0
O15	67(3)	11.0(19)	28(3)	-1(2)	0	0
O16	80(4)	14(2)	18(3)	1(2)	0	0
F1	51.9(17)	44.6(17)	40(2)	-4.1(16)	18.5(16)	-2.5(13)
F2	54.7(18)	36.7(15)	34.8(19)	-2.5(15)	-18.8(16)	-1.6(13)
F3	38.8(14)	29.4(13)	33.1(18)	1.1(13)	8.7(13)	-5.6(11)
F4	40.6(13)	27.9(13)	32.5(17)	1.9(13)	-14.1(13)	4.4(11)
F5	202(5)	32.0(18)	29(2)	-9.7(16)	-11(3)	-4(2)
F6	66(2)	118(4)	138(5)	91(4)	62(3)	61(3)
F7	29.4(13)	76(2)	54(2)	-4(2)	-3.7(15)	0.9(14)
F8	40.0(14)	27.7(13)	22.7(16)	4.7(13)	-4.8(11)	-2.4(10)
F9	87(2)	36.0(16)	36(2)	3.5(15)	-17.5(19)	-22.6(16)
F10	31(3)	51(3)	45(4)	10(3)	0(3)	6(2)
F11	41.5(19)	25.9(19)	22(2)	5.2(17)	0	0
F12	60.3(19)	40.5(16)	40(2)	-1.7(16)	-25.1(18)	0.8(14)
F13	34.1(12)	23.7(12)	29.9(17)	2.0(13)	-7.3(12)	3.1(10)

Table S4. Selected bond distances (Å) for KBOFH.

Selected bonds	Length(Å)	Selected bonds	Length(Å)
K1-F3	2.799(3)	K4-F11	2.727(4)
K1-F3 ^[3]	2.799(3)	K4-F12 ^[8]	2.928(4)
K1-F2 ^[4]	2.881(4)	K4-F12 ^[1]	2.928(4)
K1-F2 ^[5]	2.881(4)	K4-F7 ^[9]	2.651(3)
K1-O2 ^[3]	2.927(4)	K4-F7	2.651(3)
K1-O2	2.927(4)	K4-F9 ^[10]	2.884(4)
K1-O7 ^[3]	2.762(3)	K4-F9 ^[5]	2.884(4)
K1-O7	2.762(3)	K5-F13 ^[8]	2.917(4)
K2-F8 ^[15]	2.700(3)	K5-F8	2.847(3)
K2-F3 ^[16]	2.897(4)	K5-O8 ^[11]	2.905(4)
K2-F2 ^[16]	2.943(4)	K5-F12 ^[1]	3.078(4)
K2-O8 ^[17]	2.952(4)	K5-O13 ^[8]	2.802(3)
K2-O1 ^[16]	2.761(3)	K5-F7	2.939(5)
K2-O3 ^[15]	2.854(4)	K5-O3	2.923(4)
K2-O5	3.059(3)	K5-O9	2.954(3)
K2-F6	2.705(4)	K5-F9	2.718(4)
K2-F6 ^[17]	2.794(5)	K5-F5 ^[11]	3.032(5)
K3-F8 ^[5]	2.711(3)	K5-F10	3.224(7)
K3-F4 ^[16]	2.792(4)	K6-F11 ^[11]	2.851(3)
K3-F3 ^[16]	2.759(3)	K6-F4 ^[12]	2.907(4)
K3-F2 ^[18]	2.824(4)	K6-F1 ^[12]	3.117(4)
K3-F1 ^[18]	2.849(4)	K6-O1 ^[12]	2.795(3)
K3-F5	2.547(4)	K6-F7 ^[11]	3.019(4)
K3-F6 ^[15]	3.037(7)	K6-O15	2.974(4)
K4-F13 ^[6]	2.753(3)	K6-F9	2.719(4)
K4-F13 ^[7]	2.753(3)	K6-O5 ^[11]	2.911(4)

K6-O12	2.855(5)	O5-B5	1.405(7)
K6-F5 ^[11]	3.183(6)	O6-B5	1.466(6)
K6-F10 ^[11]	2.915(8)	O6-B6	1.358(7)
K7-F13 ^[10]	2.812(3)	O7-B6	1.365(7)
K7-F4 ^[13]	2.826(3)	O8-B6	1.348(7)
K7-F1 ^[14]	2.821(4)	F9-B7	1.427(7)
K7-O2 ^[13]	2.987(4)	O9-B7	1.418(11)
K7-F12	2.797(4)	O12-B7	1.461(9)
K7-O11	2.777(3)	F11-B8 ^[9]	1.409(12)
K7-O7 ^[13]	2.776(4)	F11-B8	1.409(12)
K7-O14 ^[5]	2.962(4)	O9-B8 ^[9]	1.426(12)
F1-B1	1.432(7)	O9-B8	1.426(12)
F2-B1	1.441(6)	O10-B8	1.438(11)
O1-B1	1.404(7)	O10-B8 ^[9]	1.438(11)
O4-B1	1.444(7)	F10-B8	1.467(10)
F3-B2	1.452(6)	O11-B9	1.386(9)
F4-B2	1.444(6)	O10-B9	1.361(10)
O1-B2	1.413(7)	O12-B9	1.361(9)
O2-B2	1.444(6)	O16-B10	1.445(8)
O2-B3	1.340(7)	F12-B10	1.422(6)
O3-B3	1.386(6)	O13-B10	1.418(10)
O4-B3	1.356(7)	O13-B11	1.416(10)
F5-B4	1.403(8)	O14-B11	1.454(8)
F6-B4	1.425(7)	F13-B11	1.432(6)
O5-B4	1.408(8)	O15-B12	1.371(8)
O8-B4	1.447(6)	O14-B12	1.372(10)
F7-B5	1.435(5)	O16-B12	1.348(10)
F8-B5	1.425(6)		

¹3/2-X,-1/2+Y,1/2+Z;2-1/2+X,3/2-Y,1/2+Z;³1-X,1-Y,+Z;⁴1-X,1-Y,1+Z;⁵X,+Y,1+Z;⁶3/2-X,-1/2+Y,3/2+Z;⁷X,-1/2+Y,3/2+Z;⁸+X,-1/2+Y,1/2+Z;⁹3/2-X,+Y,+Z;¹⁰3/2-X,+Y,1+Z;¹¹X,+Y,-

¹+Z;¹²+X,1/2+Y,-1/2+Z;¹³3/2-X,1/2+Y,-1/2+Z;¹⁴3/2-X,1/2+Y,1/2+Z;¹⁵1-X,3/2-Y,1/2+Z;¹⁶X,1/2+Y,1/2+Z;¹⁷1-X,3/2-Y,-1/2+Z;¹⁸+X,1/2+Y,3/2+Z

Table S5. Selected bond angles ($^{\circ}$) for $\text{K}_2\text{B}_3\text{O}_3\text{F}_4\text{OH}$.

Selected bond angles	Angle($^{\circ}$)	Selected bond angles	Angle($^{\circ}$)
F1-B1-F2	102.5(5)	F7-B5-O6	106.7(4)
F1-B1-O4	109.7(4)	O5-B5-F8	112.2(4)
O4-B1-F2	109.5(4)	O5-B5-F7	111.1(4)
O1-B1-F2	109.6(4)	O5-B5-O6	114.3(4)
O1-B1-F1	109.8(4)	O8-B6-O7	122.4(5)
O1-B1-O4	115.0(5)	O8-B6-O6	121.7(5)
F4-B2-F3	103.5(4)	O6-B6-O7	116.0(5)
O2-B2-F4	108.3(4)	B5-O5-B4	121.2(4)
O2-B2-F3	107.7(4)	B6-O6-B5	118.9(4)
O1-B2-F4	110.5(4)	B6-O8-B4	118.9(5)
O1-B2-F3	110.0(4)	O9-B7-F9 ^[10]	111.4(4)
O1-B2-O2	116.0(4)	O9-B7-O12	115.4(7)
B3-O2-B2	120.0(4)	F9 ^[10] -B7-F9	102.0(7)
B1-O1-B2	124.4(4)	F9-B7-O12	107.8(5)
B3-O4-B1	120.9(4)	F9 ^[10] -B7-O12	107.8(5)
O2-B3-O3	120.7(5)	O9-B7-F9	111.4(4)
O2-B3-O4	123.6(4)	F11-B8-O9	111.8(7)
O4-B3-O3	115.6(5)	F11-B8-O10	108.3(7)
O5-B4-O8	116.9(5)	F11-B8-F10	105.1(7)
O5-B4-F6	108.9(5)	O9-B8-O10	114.0(8)
F5-B4-O8	107.6(5)	O9-B8-F10	111.9(7)
F5-B4-O5	110.6(5)	O10-B8-F10	105.1(6)
F5-B4-F6	106.3(5)	O10-B9-O11	116.2(6)
F6-B4-O8	105.9(5)	O12-B9-O11	122.0(7)
F8-B5-F7	104.0(4)	O12-B9-O10	121.8(6)
F8-B5-O6	107.8(4)	B7-O9-B8 ^[10]	118.9(6)

B7-O9-B8	118.9(6)	F13-B11-O14	107.7(4)
B9-O10-B8 ^[10]	117.3(7)	O13-B11-F13 ^[10]	110.3(4)
B9-O10-B8	117.3(7)	O13-B11-F13	110.3(4)
B9-O12-B7	120.7(7)	O13-B11-O14	115.8(6)
O13-B10-F12	109.9(4)	F13-B11-F13 ^[10]	104.5(5)
O13-B10-F12 ^[10]	109.9(4)	O15-B12-O14	120.8(7)
O13-B10-O16	113.8(6)	O16-B12-O14	122.0(5)
F12-B10-F12 ^[10]	103.9(7)	O16-B12-O15	117.2(7)
F12 ^[10] -B10-O16	109.4(4)	B11-O13-B10	125.0(5)
F12-B10-O16	109.4(4)	B12-O14-B11	120.1(6)
F13 ^[10] -B11-O14	107.7(4)	B12-O16-B10	123.2(6)

¹3/2-X,-1/2+Y,1/2+Z; ²-1/2+X,3/2-Y,1/2+Z; ³1-X,1-Y,+Z; ⁴1-X,1-Y,1+Z; ⁵+X,+Y,1+Z; ⁶3/2-X,-1/2+Y,3/2+Z; ⁷+X,-1/2+Y,3/2+Z; ⁸+X,-1/2+Y,1/2+Z; ⁹3/2-X,+Y,1+Z; ¹⁰3/2-X,+Y,+Z; ¹¹+X,+Y,-1+Z; ¹²+X,1/2+Y,-1/2+Z; ¹³1/2+X,3/2-Y,-1/2+Z; ¹⁴3/2-X,1/2+Y,-1/2+Z; ¹⁵3/2-X,1/2+Y,1/2+Z; ¹⁶1-X,3/2-Y,1/2+Z; ¹⁷+X,1/2+Y,1/2+Z; ¹⁸1-X,3/2-Y,-1/2+Z; ¹⁹+X,+Y,2+Z; ²⁰+X,1/2+Y,3/2+Z; ²¹+X,1/2+Y,-3/2+Z; ²²3/2-X,+Y,-1+Z; ²³+X,-1/2+Y,-1/2+Z; ²⁴+X,-1/2+Y,-3/2+Z; ²⁵3/2-X,-1/2+Y,-1/2+Z

References

1. O. V. Dolomanov, L. J. Bourhis, R. J. Gildea, J. A. K. Howard and H. Puschmann, OLEX2: a complete structure solution, refinement and analysis program, *J. Appl. Crystallogr.*, 2009, **42**, 339-341.
2. G. M. Sheldrick, A short history of SHELX, *Acta Crystallogr. Sect. A.*, 2008, **64**, 112-122.
3. G. M. Sheldrick, SHELXT - Integrated space-group and crystal-structure determination, *Acta Crystallogr. Sect. A.*, 2015, **71**, 3-8.
4. A. L. Spek, Single-crystal structure validation with the program PLATON, *J. Appl. Crystallogr.*, 2003, **36**, 7-13.
5. B. E. Sorensen, A revised Michel-Levy interference colour chart based on first-principles calculations, *Eur. J. Mineral.*, 2013, **25**, 5-10.
6. L. L. Cao, G. Peng, W. B. Liao, T. Yan, X. F. Long and N. Ye, A microcrystal method for the measurement of birefringence, *CRYSTENGCOMM*, 2020, **22**, 1956-1961.
7. S. J. Clark, M. D. Segall, C. J. Pickard, P. J. Hasnip, M. J. Probert, K. Refson and M. C. Payne, First principles methods using CASTEP, *Z. Kristalloger.*, 2005, **220**, 567-570.
8. M. C. Payne, M. P. Teter, D. C. Allan, T. A. Arias and J. D. Joannopoulos, Iterative minimization techniques for ab initio total-energy calculations - molecular-dynamics and conjugate gradients, *Rev. Mod. Phys.*, 1992, **64**, 1045-1097.
9. W. Kohn and L. J. Sham, Self-consistent equations including exchange and correlation effects, *Phys. Rev.*, 1965, **140**, 1133-&.
10. J. P. Perdew, K. Burke and M. Ernzerhof, Generalized gradient approximation made simple (vol 77, pg 3865, 1996), *Phys. Rev. Lett.*, 1997, **78**, 1396-1396.
11. A. M. Rappe, K. M. Rabe, E. Kaxiras and J. D. Joannopoulos, Optimized pseudopotentials, *Phys. Rev. B*, 1990, **41**, 1227-1230.
12. H. J. Monkhorst and J. D. Pack, Special points for brillouin-zone integrations, *Phys. Rev. B*, 1976, **13**, 5188-5192.